Journal of Alloys and Compounds 522 (2012) 118–122

Contents lists available at SciVerse ScienceDirect

Journal of Alloys and Compounds

journal homepage: www.elsevier.com/locate/jallcom

Fabrication and performance of N-doped ZnO UV photoconductive detector

S.S. Shinde, K.Y. Rajpure*

Electrochemical Materials Laboratory, Department of Physics, Shivaji University, Kolhapur 416004, India

A R T I C L E I N F O

Article history:
Received 25 November 2011
Received in revised form 16 January 2012
Accepted 18 January 2012
Available online 28 January 2012

Keywords:
Spray pyrolysis
Ultraviolet photodetector
N:ZnO
Alumina
ZnO buffer layer

A B S T R A C T

We report study on the fabrication and characterization of an ultraviolet (UV) photodetectors based on N-doped ZnO films. The N-doped ZnO films with 10 at% N doping are spray deposited on to alumina substrates. The photoconductive UV detector based on N-doped ZnO thin films, having a metal–semiconductor–metal (MSM) configuration are fabricated using Al as a contact metal. The dependence of *I*–*V* characteristic under dark and illumination, spectral and transient photoresponse of the detector are investigated. The linear current–voltage (*I*–*V*) characteristics under forward bias exhibit ohmic metal–semiconductor contact. The UV photoconductive effect is observed showing fast response with switching on/off UV light illumination. The neutralization of photogenerated holes by negatively charged oxygen ion plays a key role in the photoconductive characteristics of N-doped ZnO polycrystalline films.

© 2012 Elsevier B.V. All rights reserved.

1. Introduction

Various binary and ternary oxide semiconductors have been of growing interest recently as potential candidates for application in ultraviolet optoelectronic technologies. Wurtzite (hexagonal) structured zinc oxide (ZnO) is a wide band gap semiconductor and is a chemically and thermally stable material. Due to wide-band gap, ZnO is a promising material and has been used in various devices such as surface acoustic wave devices, pyroelectric devices, gas sensors, varistors and transparent electrodes [1–6]. Moreover, ZnO holds a strong potential candidate for light-emitting diodes (LEDs), laser diodes (LDs) and ultraviolet (UV) detecting devices [7–12]. UV detection has many important applications, including satellite-based missile plume detection, air quality monitoring, environment monitoring, space research and high temperature flame detection [3]. There are various types of UV detectors: metal–semiconductor–metal (MSM) detector, Schottky photodiode [13], p–n photodiode and so on. Among them, the MSM structured photoconductive detector with two ohmic contacts is generally the simplest detectors to grow and fabricate. Over the past few years, there have been some demonstrations about ZnO-based MSM photoconductive detectors [14–18]. Li et al. [7] and Liang et al. [4] made UV photodetectors using ZnO epitaxial films grown on sapphire by MOCVD. Liu and Kim [9] investigated UV detection properties of ultrathin ZnO epitaxial films grown on c-plane sapphire substrates with radio frequency (rf) magnetron sputtering technique. Fabricius et al. [19] studied UV-sensitive photodiodes using Schottky barrier formed in the contact layer between a thin sputtered layer of ZnO and Au. High-quality ZnO films were epitaxially grown on R-plane sapphire substrates by MOCVD at temperatures in the range of 350–600 °C by Liu et al. [20]. The MSM ultraviolet sensitive photodetectors were fabricated on N-doped epitaxial ZnO films. The detector showed fast photoresponse of the order of 400 A/W at 5 V bias. Till today, there are no reports on the N-doped ZnO UV detectors with ZnO as buffer layer thin films grown on alumina substrates. In this paper, we report the preparation and photoelectric properties of the N-doped ZnO photoconductive ultraviolet detectors using ZnO buffer films grown on alumina substrates by spray pyrolysis.

2. Experimental

The 0.1 M zinc acetate ($Zn(CH_3COO)_2 \cdot 2H_2O$) Aldrich, 99.99%, A.R. grade) is dissolved in double distilled water. The resulting 100 cm^3 solution was sprayed onto cleaned alumina substrates at 450 °C. This layer of thickness ~200 nm acts as buffer layer. Then N-doped ZnO layer (using AR grade zinc acetate and N,N Dimethyl Formamide as precursors) was grown in aqueous medium on to the ZnO buffer layer for photodetector devices. The doping percentage of dopant (N,N dimethyl formamide) in the solution [N/Zn] was 10 at%. The alumina substrate was cleaned ultrasonically to remove surface contaminants, which was followed by rinsing in double-distilled water. Then substrates were dried in methanol vapour. The typical spray parameters such as spray rate (5 cm^3/min), substrate temperature (450 °C), solution concentration (0.1 M), quantity (100 cm^3), substrate to nozzole distance (30 cm) were kept constant in throughout device fabrication process. The ambient air was used as carrier gas.

Photoconductive UV detector device was fabricated using conventional spray pyrolysis techniques based on metal–semiconductor–metal (MSM) configuration. The ohmic contacts were made by Al metal foil onto the N-doped zinc oxide layer. The cross-sectional device structure is illustrated in Fig. 1. The optical reflection spectrum was recorded using a StellerNet Inc USA reflectometer. Current–voltage

* Corresponding author. Tel.: +91 231 2609435; fax: +91 231 2691533.
E-mail address: rajpure@yahoo.com (K.Y. Rajpure).

0925-8388/$ – see front matter © 2012 Elsevier B.V. All rights reserved.
doi:10.1016/j.jallcom.2012.01.118

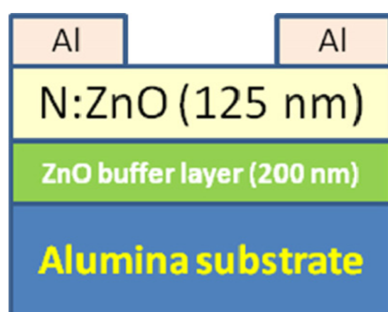

Fig. 1. Schematic structural configuration of the fabricated N-doped ZnO photoconductive detector device onto the alumina.

(I–V) characteristic was recorded by sweeping the bias voltage from 0 to 5 V across the junction using AMEL instruments model 2059 electrometer. Before the dark I–V measurement, the sample was kept in the dark for more than 24 h to stabilize the dark current. DC photocurrents were measured by illuminating the sample with an OMNILUX UV source (made in France). The wavelength was varied from 350 to 450 nm using a monochromator at a fixed bias of 5 V. Special care was taken to determine the dark current after waiting for long time (h). All measurements were made at room temperature.

3. Results and discussion

Fig. 2(a) shows the core level XPS spectra of typical 10 at% NZO thin film. The doublet line of Zn corresponding to $2p_{3/2}$ and $2p_{1/2}$ are observed at 1022.2 and 1045.3 eV, respectively. The Zn ($2p_{3/2}$) line has been shifted by ΔE_{Zn} = 0.7 eV from the binding energy position of 1021.5 eV for elemental zinc [21]. Fig. 2(b) shows O 1s core level XPS spectra of typical 10 at% NZO thin film. The O1s peak is broad and asymmetric. The spectrum shows mainly a peak at 531 eV with splitting at about 532.5 and 530 eV. The peak is assigned to oxygen atoms bound to Zn in ZnO. The N-doped film shows O 1s peak at 531 eV due to the contribution of N—O bonds as well as that of ZnO. The stronger peak at 530 eV may be attributed to O^{2-} ions in Zn—O bonds, while another peak at 532.5 eV is usually associated with the loosely bound oxygen (e.g. adsorbed O_2, —OH) chemisorbed on the surface and grain boundary of polycrystalline film [22]. Fig. 2(c) shows the N 1s core level spectra of typical 10 at% N doped ZnO thin film. The literature shows that the binding energy of the N 1s line is very sensitive to the chemical environment of the nitrogen atom. One peak of binding energy at about ∼400 eV which corresponds to the N 1s core level is observed. This is attributed to presence of N—Zn bond in NZO film [23,24].

Fig. 3 shows the reflectance spectra of pure and typical 10 at% N-doped ZnO photodetector thin films. It reflects the real reflection characteristic of N-doped ZnO thin film photodetector excluding substrate contribution. The average reflectance increases due to nitrogen doping. The dark and photo-illuminated current–voltage (I–V) characteristics of pure and N-doped ZnO detector fabricated onto alumina substrate are shown in Fig. 4. The performance of the detector has been evaluated using Al/(ZnO and N:ZnO)/Al MSM structural configuration. The linear I–V (current–voltage) relation under forward bias exhibits the ohmic contact of the photoconductive detector. The detector operates in photoconductive mode with wavelength 365 nm and power (2 μW) of illuminated light for measurement of current–voltage characteristic. The observed dark current is about 16 and 8 μA at 5 V bias for pure and N:ZnO detector. This indicates that film has many intrinsic donor defects, such as oxygen vacancies and zinc interstitials. It has tendency to lose its oxygen atoms and become non-stoichiometric [25]. In the dark, oxygen is adsorbed by taking a free electron from film in presence of air, leaving a depletion region near the surface and grain boundaries. The negative oxygen ions adhere to the surface and crystallite interfaces of the film and form a chemically adsorbed

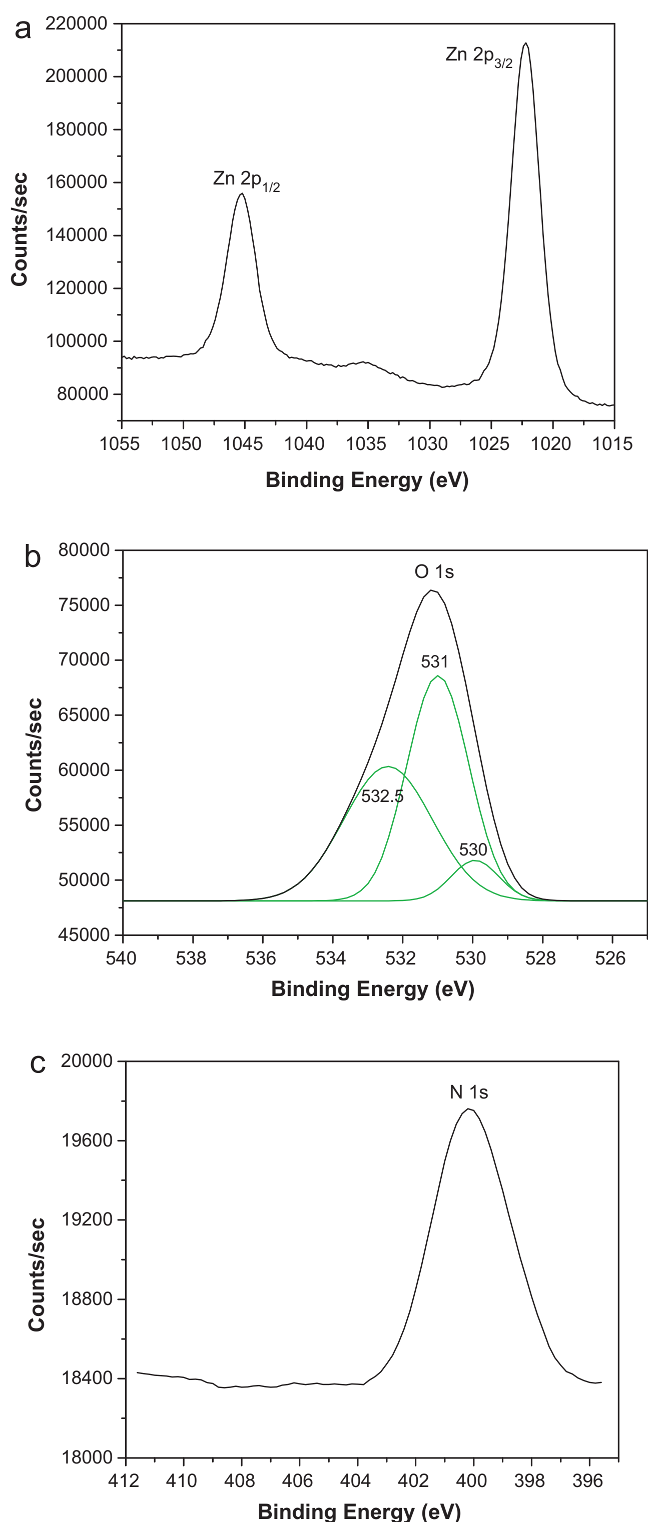

Fig. 2. Narrow scan XPS spectra of (a) Zn 2p, (b) O 1s, and (c) N 1s core levels for 10 at% N-doped ZnO thin film.

surface state. These oxygen ions are bound carriers and cannot contribute to the conductivity of film. The adsorption of oxygen also introduces potential barrier, which is unfavorable for the carrier mobility. The N-doped ZnO crystallite interface exist double depletion barrier [26]. Conductivity is a product of the carrier density and mobility, so dark conductivity of our detector is small as a result of oxygen adsorption. The current increases greatly when

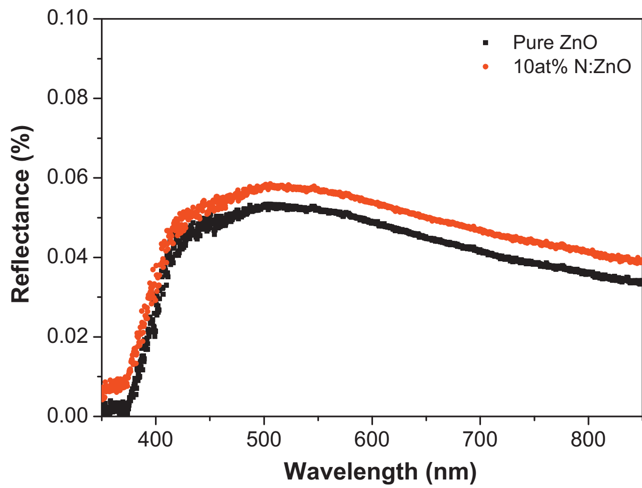

Fig. 3. The reflectance spectra of pure and N-doped ZnO photoconductive detector.

switching on the UV light compared with dark at high bias, indicating the high UV-sensitive photoconductivity. Under UV illumination using monochromatic light with a wavelength of 365 nm photo-generated current is 0.346 (ZnO) and 1.06 mA (NZO/ZnO) at 5 V bias. While under UV light illumination electron and hole pairs are generated. Photogenerated holes are captured by the negatively charged oxygen ions and leave excess conduction-band electrons. The oxygen photodesorption also lowers the barrier height of grain-boundaries and increases carrier mobility as a result conductivity increases. Compared with ZnO polycrystalline films, high-quality N-doped ZnO epitaxial films have few grain boundaries so that such large photocurrent with weak incident power has been observed. In conclusion, the detector shows large photocurrent due to the accumulation of non-equilibrium electrons in the conduction band and decrease in barrier height between crystallites, accompanied with the photogenerated holes captured by the negatively charged oxygen ions.

Fig. 5 shows the dependence of photocurrent as a function of optical power density at a wavelength of 365 nm for pure and 10 at% N:ZnO detector. Thermal effects have been neglected because of weak power of the source. The photocurrent increases linearly with incident power density. No obvious saturation is observed in our measured range, indicating its suitability for practical use. Upon UV illumination (~365 nm, 2 μW) the photocurrent increased from 0.346 to 1.06 mA at 5 V bias due to N doping, showing high responsivity.

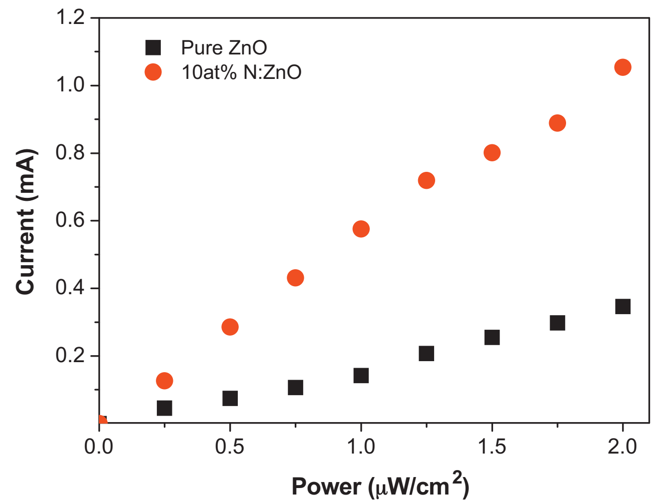

Fig. 5. Dependence of photocurrent with optical power density of the pure and N-doped ZnO photoconductive detector at 5 V bias.

Fig. 6 shows the spectral response of Al/(ZnO and N-doped ZnO)/Al MSM photodetector. The photocurrent increases with respect to wavelength up to 365 nm and then falls sharply in the visible region. When the wavelength decreases, absorption coefficient will increase and penetration depth of UV light will be shallower, thus carrier concentration increases near the film surface. As a result, lifetime of photogenerated carriers will decrease and lead to drop in responsivity. A sharp cutoff near 373 nm is observed. The photoresponse drops considerably across the cutoff wavelength within 16 nm of the band edge. The photoresponsivity is more than 5 times larger below 365 nm than in the visible range, indicating that a photoconductivity UV detector with high sensitivity has been made. The large photocurrent density as well as responsivity can be ascribed to much more carriers collected under illumination with nitrogen doping in the ZnO thin films. The response in the UV region is due to band-to-band transitions of N-doped ZnO thin film and a tail of response near the band edge indicates defect distributed in the film such as dopants, or defects localized in lattice discontinuities (dislocations, grain boundaries and interfaces) [27,28].

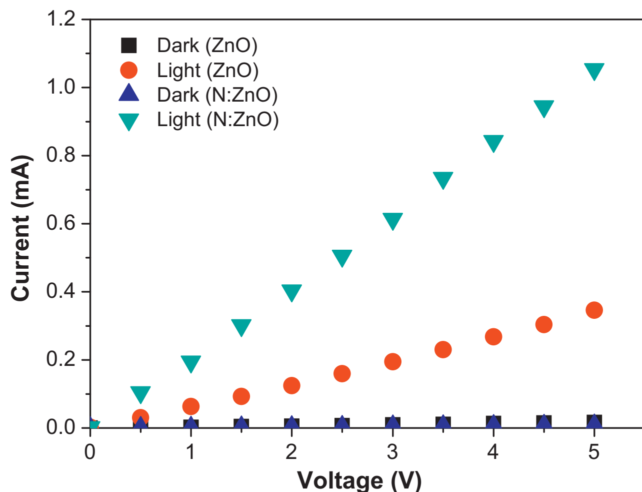

Fig. 4. *I–V* characteristics of the pure and N-doped ZnO photoconductive detector, showing dark current and photocurrent at 365 nm.

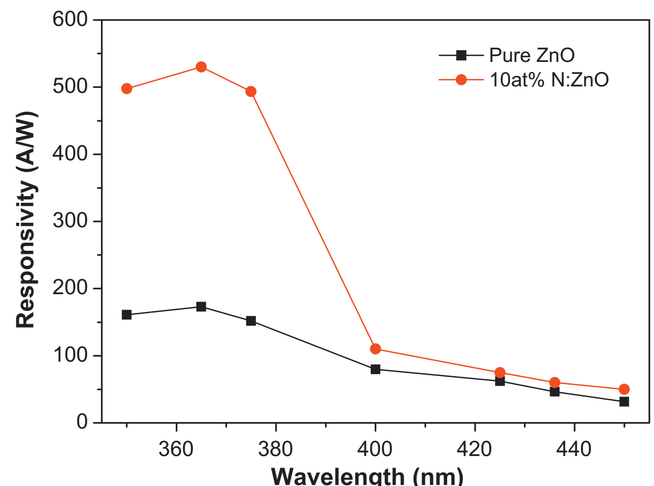

Fig. 6. Spectral response of the pure and N-doped ZnO photodetector at 5 V bias.

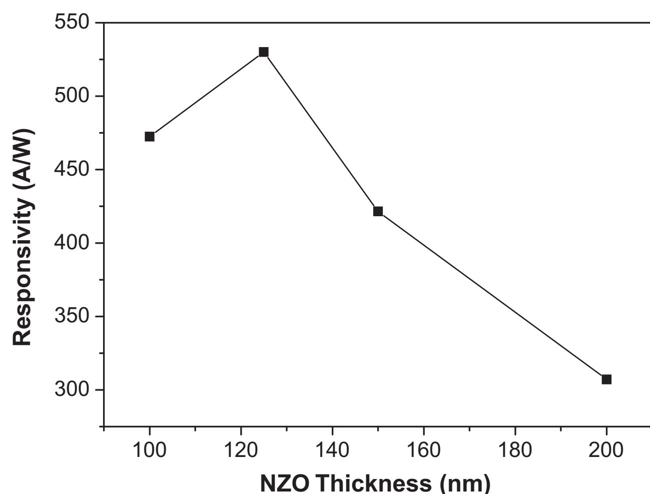

Fig. 7. Plot of thickness against responsivity of the N-doped ZnO photodetector at 5 V bias.

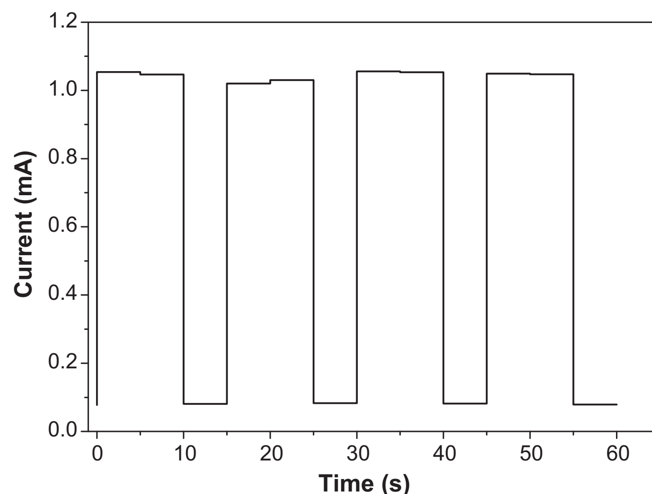

Fig. 9. Photocurrent as a function of time as obtained by switching on and off UV light (2 mW/cm^2) illumination on the UV photodetector from N-doped ZnO film at 5 V bias.

This growth mechanism may produce numerous nuclei sites on alumina surface layer and thus promote the subsequent growth of the ZnO buffer layer. Since the three-dimensional growth of ZnO buffer layer is dominant as compared to the islands expanding laterally and coalescing, the lower nuclei density and higher height of nuclei can be achieved in the ZnO buffer layers on the alumina surface. As a result, we can reduce grain boundaries and thus achieve a larger volume of defect-free regions using ZnO buffer layer. With increasing growth time of ZnO layer, more and more nuclei sites are formed. The crystal quality of NZO epitaxial layer could be more improved by increasing growth time. Fig. 7 shows the variation of responsivity versus thickness of the N:ZnO layer. It is seen that responsivity increases with increase in thickness up to 125 nm and then decreases for higher thickness. Variation of spectral responsivity w. r. t. doping concentration (Fig. 8) confirms the responsivity increases with N doping concentration up to 10 at% attaining maximum 530 A/W value and further decreases for higher doping concentrations. This attributes to change in metastable N-on-O substitution (N_O), which may attract another N to form a $(N_2)_O$ donor or leave the O site to diffuse in the ZnO, at the same time, generate a V_O donor [29]. Generally, nitrogen can be substituted inside the ZnO in two forms: atomic nitrogen on oxygen sites (N_O) acting as acceptors and molecular nitrogen on oxygen sites $(N_2)_O$ acting as donors. Formation enthalpy of $(N_2)_O$ is lower than (N_O) which

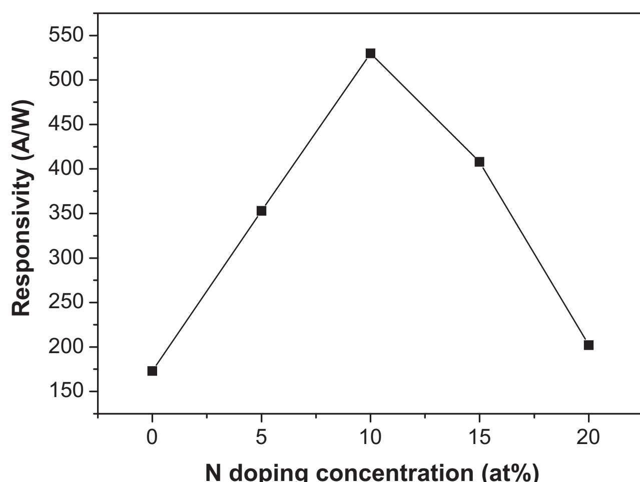

Fig. 8. Variation of responsivity of N:ZnO detector w. r. t. N-doping concentration.

leads to n type conduction of NZO thin films. The N—N atoms have strong bonding energy compared to N—Zn bonding energy [30,31]. The improvement in photoresponsivity of doped thin films is due to morphological modifications that enhance the active surface area and quenching of defect levels responsible for recombination losses, as compared to the pure ZnO. The present results are better than the results reported by Liu et al. [20], who have reported the responsivity to be 400 A/W (at 5 V bias) for MOCVD prepared epitaxial NZO films. Sun et al. [32] reported the maximum responsivity of the ZnO *p–i–n* structured photodetector, which is located at around 390 nm, is about 0.45 mA W^{-1} at 0 V bias, and the responsivity increases with increasing reverse bias voltage applied.

The reproducibility of the device is also ensured by cyclically switching UV light on and off for same time intervals. As shown in Fig. 9, current of the device could be reversibly modulated by UV irradiation. As the device is illuminated by UV light, current increases sharply and remains stable under steady light. When light source is removed then it recovers to initial value. The peak value of photocurrent with incident power of 2 μW is 1.06 mA, which is much larger than reported detectors fabricated on high-quality epitaxial ZnO films [4,14]. It shows very good reproducibility for at least 50 times without much change, indicating good stability for the device. This result also indicates that the UV sensing mechanism involves some reversible interactions between the N-doped ZnO and UV light.

4. Conclusions

We have investigated the photoconductive properties of pure and N-doped ZnO films fabricated on alumina for fast UV photodetectors and optoelectronic applications. The linear current–voltage (*I–V*) characteristics under forward and reverse bias exhibit ohmic metal–semiconductor contact. The maximum photocurrent of detector is observed to be 1.06 mA at 365 nm for 5 V bias. The fabricated UV detector exhibits highest spectral responsivity of about 530 A/W for 5 V bias. From this, it is confirmed that N-doped ZnO is promising material to produce cost-effective devices with higher responsivity.

Acknowledgement

The authors are very much thankful to the Defense Research and Development Organization (DRDO), New Delhi, for the financial support through its project No. "ERIP/ER/0503504/M/01/1007".

References

[1] T. Aoki, Y. Hatanaka, D.C. Look, J. Appl. Phys. 76 (2000) 3257.
[2] S. Yata, Y. Nakashima, T. Kobayashi, Thin Solid Films 445 (2003) 259–262.
[3] D. Basak, G. Amin, B. Mallik, G.K. Paul, S.K. Sen, J. Cryst. Growth 256 (2003) 73–77.
[4] S. Liang, H. Sheng, Y. Liu, Z. Huo, Y. Lu, H. Shen, J. Cryst. Growth 225 (2001) 110–113.
[5] W. Yang, R.D. Vispute, S. Choopun, R.P. Sharma, T. Venkatesan, H. Shen, Appl. Phys. Lett. 78 (2001) 2787–2789.
[6] S.S. Shinde, P.S. Patil, R.S. Gaikwad, R.S. Mane, B.N. Pawar, K.Y. Rajpure, J. Alloys Compd. 503 (2010) 416.
[7] Y. Li, F.D. Valle, M. Simonnet, I. Yamada, J.J. Delaunay, Nanotechnology 20 (2009) 045501.
[8] H.S. Bae, S. Im, Thin Solid Films 469 (2004) 75–79.
[9] M. Liu, H.K. Kim, Appl. Phys. Lett. 84 (2004) 173–175.
[10] S.S. Shinde, C.H. Bhosale, K.Y. Rajpure, Solid-State Electronics 68 (2012) 22.
[11] S.S. Shinde, K.Y. Rajpure, Mater. Res. Bull. 46 (2011) 1734.
[12] S.S. Shinde, K.Y. Rajpure, Appl. Surf. Sci. 257 (2011) 9595.
[13] Y.Z. Li, X.M. Li, X.D. Gao, J. Alloys Compd. 509 (2011) 7193.
[14] Q.A. Xu, J.W. Zhang, K.R. Ju, X.D. Yang, X. Hou, J. Cryst. Growth 289 (2006) 44–47.
[15] Z.Q. Xu, H. Deng, J. Xie, Y. Li, X.T. Zu, Appl. Surf. Sci. 253 (2006) 476–479.
[16] K.W. Liu, J.G. Ma, J.Y. Zhang, Y.M. Lu, D.Y. Jiang, B.H. Li, D.X. Zhao, Z.Z. Zhang, B. Yao, D.Z. Shen, Solid-State Electron. 51 (2007) 757–761.
[17] K.J. Chen, F.Y. Hung, S.J. Chang, S.J. Young, J. Alloys Compd. 479 (2009) 674.
[18] P.C. Chang, Y.K. Su, K.J. Lee, C.L. Yu, S.J. Chang, C.H. Liu, J. Alloys Compd. 504 (2010) S429.
[19] H. Fabricius, T. Skettrup, P. Bisgaard, Appl. Optics 25 (1986) 2764.
[20] Y. Liu, C.R. Gorla, S. Liang, N. Emanetoglu, Y. Lu, H. Shen, M. Wraback, J. Electron. Mater. 29 (2000) 69.
[21] B.A. de Angelis, J. Electron Spectrosc. Relat. Phenom. 9 (1976) 81.
[22] M. Chen, X. Wang, Y.H. Yu, Z.L. Pei, X.D. Bai, C. Sun, R.F. Huang, L.S. Wen, Appl. Surf. Sci. 158 (2000) 134.
[23] C.L. Perkins, Se-Hee Lee, Xiaonan Li, Sally E. Asher, Timothy J. Coutts, J. Appl. Phys. 97 (2005) 034907.
[24] X. Yang, A. Wolcott, G. Wang, A. Sobo, R.C. Fitzmorris, F. Qian, J.Z. Zhang, Y. Li, Nano Lett. 9 (2009) 2331–2336.
[25] Z.Y. Xue, D.H. Zhang, Q.P. Wang, J.H. Wang, Appl. Surf. Sci. 195 (2002) 126–129.
[26] T.L. Tansley, D.F. Neely, Thin Solid Films 121 (1984) 95–107.
[27] H.Z. Xu, Z.G. Wang, M. Kawabe, I. Harrison, B.J. Ansell, C.T. Foxon, J. Cryst. Growth 218 (2000) 1–6.
[28] P. Sharma, K. Sreenivas, K.V. Rao, J. Appl. Phys. 93 (2003) 3963–3970.
[29] L.G. Wang, A. Zunger, Phys. Rev. Lett. 90 (2003) 256401.
[30] Q. Ou, K. Shinji, A. Ogino, M. Nagatsu, J. Phys. D: Appl. Phys. 41 (2008) 205104.
[31] S. Limpijumnong, X.N. Li, S.H. Wei, S.B. Zhang, Appl. Phys. Lett. 86 (2005) 211910.
[32] F. Sun, C.X. Shan, S.P. Wang, B.H. Li, Z.Z. Zhang, C.L. Yang, D.Z. Shen, Mater. Chem. Phys. 129 (2011) 27–29.